Supporting information for

Efficient and Reusable Catalysis of Benzylic C-H Oxidation over Layered $[Co_5(OH)_6]^{4+}$ Derivatives

Wen Ma,‡ Chengdong Peng,‡ Xueling Song, Lu Zhang and Honghan Fei*

Shanghai Key Laboratory of Chemical Assessment and Sustainability, School of Chemical Science and Engineering, Tongji University, 1239 Siping Rd., Shanghai 200092, P. R. China.

‡ These authors contributed equally.

* Corresponding Author: fei@tongji.edu.cn

Experimental Section

Materials

$Co(OH)_2$ (99.0%, Aladdin), $Ni(OH)_2$ (98.0%, TCI), adipic acid (99%, TCI), sodium dodecyl sulfate (SDS, 93%, Sigma-Aldrich), Na_2SO_4 (99%, Adamas), $NaClO_4$ (99%, Adamas), NaCl (99.99%, Adamas), Na_2CO_3 (99%, Adamas), Na_3PO_4 (99%, Adamas), ethylbenzene (99%, Adamas), tetralin (98%, Adamas), *tert*-butyl hydroperoxide (70% solution in water, Adamas), ethanol (99.7%, Greagent) were used as received without further purification. Deionized water was obtained from a Barnstead Pacific RO water purification system.

Solvothermal Synthesis of TJU-28.

0.5 g $Co(OH)_2$ and 0.4 g adipic acid were adequately dispersed in 10 mL deionized water by magnetic stirring for 15 min, followed by transferring the mixtures into a 15 mL Teflon-lined autoclave and heating statically at 200 °C for 72 h. After 72 h, the autoclave was cooled down to room temperature. The purple plate-shaped crystals of TJU-28(Co) were isolated by vacuum filtration, then washed with deionized water and ethanol for several times, and dried under vacuum at 70 °C. The high phase purity was confirmed by comparing experimental PXRD patterns with theoretical pattern simulated from the single-crystal X-ray diffraction data. Anal. cal. for $[Co_{2.5}(OH)_3][(CH_2)_4(COO)_2]$: calculated: C, 21.04%, H, 3.24%; observed: C, 21.05%, H, 3.23%. Isostructural synthesis of TJU-28(Ni), TJU-28($Co_{0.95}Ni_{0.05}$) and TJU-28($Co_{0.9}Ni_{0.1}$) were performed under the same reaction conditions but using $Ni(OH)_2$, $Co(OH)_2$:$Ni(OH)_2$=9.5:0.5, and $Co(OH)_2$:$Ni(OH)_2$=9:1 and $Co(OH)_2$:$Ni(OH)_2$=9.5:0.5 in place of $Co(OH)_2$ during solvothermal synthesis.

Synthesis of TJU-28(Co) Nanosheets.

100 mg of the as-synthesized TJU-28(Co) crystals were dispersed in 20 mL of ethanol containing 0.5767 g of SDS to obtain a uniform suspension under ultrasonic condition for 5 min. After this system was incubated at 60 °C for 24 h, the suspension was centrifuged and washed with DI water for 3 times. The obtained products were dispersed in 20 mL of DI water, and placed onto a shaker (160 rpm) under room temperature for 3-6 hours. Then, the suspension was centrifuged and dispersed in 20 mL of ethanol, and followed by placing onto a shaker (160 rpm) under room

temperature for 12 hours. Finally, the nanosheets were isolated from the supernatant *via* centrifugation and washed with mixed water/ethanol (v/v=1:1) solution for 3 times, and then dried under vacuum. The element analysis indicated the TJU-28(Co) nanosheets have a molecular formula of $Na_2[Co_5(OH)_8(adipate)(SDS)_{0.4}]$. Anal. cal. for $Na_2[Co_5(OH)_8(adipate)(SDS)_{0.4}]$: calculated: C, 17.62%; H, 3.56%; S, 1.74%; observed: C, 17.94%; H, 3.48%; S, 1.68%.

Single Crystal X-ray Diffraction (SCXRD).

A single crystal of TJU-28(Co) suitable for X-ray analysis was chosen under an optical microscope (NIKON ECLIPSE LV100N POL), and carefully mounted onto a glass fiber. The crystal structure of the as-prepared single crystal was analyzed by a Bruker SMART APEX II CCD area detector X-ray diffractometer, applying a graphite-monochromatic Mo-Kα radiation (λ= 0.71073 Å) from a fine-focus sealed tube operated at 50 kV and 30 mA. Diffraction data were processed with the APEX3 software package, integrated using SAINT, and further corrected for absorption effects using SADABS. Space-group was determined by systematic absences, E-statistics, agreement factors for equivalent reflections, and successful refinement of the structure. An empirical absorption correction was applied. The data were corrected for Lorentz-polarization effects. The crystal structure was solved by direct methods and expanded routinely. The model was refined by full-matrix least-squares analysis of F^2 against all reflections. All non-hydrogen atoms were refined with anisotropic thermal displacement parameters. Thermal parameters for hydrogen atoms were tied to the isotropic thermal parameter of the atom to which they are bonded. The used programs included APEX-II v2.1.4,[S1] SHELXTL v6.14,[S2] and DIAMOND v3.1e.[S3] Further details of crystallographic data and structural refinement are summarized in Table S1. Simulated powder patterns were calculated by Mercury software applying the crystallographic information from the SCXRD results.

Instrumental Characterization.

Powder X-ray Diffraction (PXRD) analysis was performed using on a BRUKER D2 PHASER X-ray diffractometer equipped with a Cu sealed tube (λ= 1.54184 Å) at 30 kV and 10 mA. The diffraction patterns were scanned at ambient temperature, with a scan speed of 1 sec/step, a step size of 0.02° in 2θ, and a 2θ range of 5 ~ 40°. Simulated powder patterns were calculated by Mercury software using the crystallographic information file from the Cambridge Crystallographic Data

Center. FT-IR spectrum were recorded using a BRUKER ALPHA spectrophotometer with a wavenumber range of 4000 ~ 400 cm^{-1} with a resolution of 2 cm^{-1}. Elemental analysis (EA) for C/H/N/S was performed in a Varian EL III element analyzer. X-ray photoelectron spectroscopy (XPS) for elemental analysis was conducted on a Kratos Axis Ultra DLD X-ray Photoelectron Spectrometer using 100 W monochromated Al Kα radiation as the X-ray source for excitation. The 500 μm X-ray spot was used for XPS analysis. The base pressure in the analysis chamber was about 3×10^{-10} mbar. The C 1*s* peak (284.8 eV) was used for internal calibration. The peak resolution and fitting were processed with the XPS Peak 41 software. TGA analysis was carried out on a TGA Q5000 differential thermal analyzer. The samples were heating in N_2 stream from 25 to 800 °C with a heating rate of 10 °C min^{-1}. Transmission electron microscopy (TEM) images were captured on a JEOL JEM2100F microscopy, using the electronic diffraction attachment to take a SAED (selected area electronic diffraction) picture. Scanning electron microscopy (SEM) was carried out on a Pheom Pro instrument using a 10 kV energy source under vacuum. The thickness of the TJU-28(Co) nanosheets was measured precisely on a tapping-mode atomic force microscopy (AFM, Bruker multimode 8). Co leaching in catalytic reactions and Ni incorporation in the synthesis were measured on a PerkinElmer Optima 8300 ICP-OES.

X-ray absorption fine structure spectroscopy (XAFS) and data analysis

X-ray absorption find structure spectra (Co K-edge) were collected at BL14W1 station in Shanghai Synchrotron Radiation Facility. Data reduction, data analysis, and EXAFS fitting were performed with the Athena and Artemis software packages.[s4] The energy calibration of the sample was conducted through a standard Co foil, which as a reference was simultaneously measured. A linear function was subtracted from the pre-edge region, then the edge jump was normalized using Athena software. The χ(k) data were isolated by subtracting a smooth, three-stage polynomial approximating the absorption background of an isolated atom. The k3-weighted χ(k) data were Fourier transformed after applying a Hanning window function (Δk = 1.0). For EXAFS modeling, the global amplitude EXAFS (CN, R, S_0^2, σ^2 and ΔE_0) were obtained by nonlinear fitting, with least-squares refinement, of the EXAFS equation to the Fourier-transformed data in R-space, using Artemis software, EXAFS of the Co foil is fitted and the obtained amplitude reduction factor S_0^2 value (0.816) was set in the EXAFS analysis to determine the coordination numbers (CNs) in the Co-O/Co scattering path in sample. For Wavelet Transform analysis, the χ(k) exported from Athena

was imported into the Hama Fortran code.[S5] The parameters were listed as follow: R range, 1~3.5 Å, k range, 0~13.0 $Å^{-1}$ for Co1/2 (0~13.0 $Å^{-1}$ for Co foil and $Co(OH)_2$); k weight, 2; and Morlet function with $\kappa=10$, $\sigma=1$ was used as the mother wavelet to provide the overall distribution.

Chemical and Thermal Stability Studies

~100 mg of the as-synthesized materials were incubated in various solvent (H_2O, CH_3CN, CH_2Cl_2, CH_2OH, DMF) for 24 h before performing PXRD measurements. Thermal stability experiments were carried out by incubation of TJU-28 in an oven at 150 °C for 12 h. PXRD characterizations were performed after cooling to the room temperature.

Benzylic C-H Oxidation Catalysis

The solvent-free aerobic oxidation of ethylbenzene and tetralin were performed in an autoclave with magnetic stirring. Typically, the substrate, catalyst, initiator and oxygen were mixed in the reactor by magnetic stirring for 5 min at room temperature. Then, the reaction system was heated to a given temperature (the temperature was measured with a thermometer in an oil bath). After the reaction, the product was taken out from the reaction system and the conversions were checked by gas chromatography-mass spectrometry (GC-MS, Shimadzu GCMS−QP2010 SE) using naphthalene as the internal standard. The typical reaction condition: 8 mmol of substrate, 50 mg catalyst, 12 h reaction time, 100 °C for ethylbenzene and 120 °C tetralin. 66 μL *t*-butyl hydroperoxide (TBHP) was added as the initiator. The recyclability of the catalyst was tested by separation of catalysts by centrifugation, washing with ethanol and drying at 80 °C.

Supporting Tables and Figures

Table S1. Crystal data and structure refinement of TJU-28(Co).

Identification code	TJU-28(Co)
Empirical formula	$C_6H_{11}Co_{2.5}O_7$
Formula weight	342.47
Temperature/K	293(2)
Crystal system	triclinic
Space group	*P*-1
Unit cell dimensions	*a*/Å=6.288(3), *b*/Å=6.990(3), *c*/Å=11.658(5) *α*/°=83.368(5), *β*/°=80. 845(4), *γ*/°=73.214(4)
Volume/Å^3	490.7(4)
Z	2
ρ_{calc}/g•cm^{-3}	2.318
μ/mm^{-1}	4.210
F(000)	341.0
Crystal size/mm^3	0.3 × 0.22 × 0.02
2θ range for data collection/°	6.1 to 56.44
Index ranges	$-8 \le h \le 8$, $-9 \le k \le 9$, $-15 \le l \le 12$
Reflections collected	3084
Independent reflections	2148 [R_{int}=0.1429, R_{sigma}=0.1838]
Data/restraints/parameters	2148/3/155
Goodness-of-fit on F^2	1.018
Final R indexes [I>=2σ (I)]	R_1 = 0.0791, wR_2 = 0.1911
Final R indexes [all data]	R_1 = 0.1233, wR_2 = 0.2100
Largest diff. peak/hole (e Å^{-3})	1.50/-2.06

$R_1=\Sigma(||F_o|-|F_c||)/\Sigma|F_o|$; $wR_2=\{\Sigma[w(F_o^2-F_c^2)^2]/\Sigma[w(F_o^2)]^2\}^{1/2}$

Table S2. Synthetic conditions and the observed Ni wt.‰ in TJU-28(Co/Ni).

Sample	TJU-28($Co_{0.95}Ni_{0.05}$)	TJU-28($Co_{0.9}Ni_{0.1}$)
Calculated molar ratio (Co:Ni)	19	9
Observed molar ratio (Co:Ni) by ICP-OES	18.21	11.10

Table S3. EXAFS fitting parameters at the Co K-edge for various samples (S_0^2=0.816).

Sample	Shell	*CN* [a]	*R*(Å) [b]	σ^2(Å^2) [c]	ΔE_0(eV) [d]	*R* factor
Co foil	Co-Co	12*	2.49±0.01	0.0063±0.0004	6.9±0.5	0.0027
$Co(OH)_2$	Co-O	6.1±0.4	2.10±0.01	0.0079±0.0011	1.3±0.6	0.0057
TJU-28(Co) bulk	Co-O	6.0±0.6	2.07±0.01	0.0084±0.0015	-3.2±4.7	0.0053
TJU-28(Co) nanosheets	Co-O	5.1±0.7	2.07±0.01	0.0101±0.0024	-1.5±1.2	0.0061

[a]*CN*, coordination number; [b]*R*, distance between absorber and backscatter atoms; [c]σ^2, Debye-Waller factor to account for both thermal and structural disorders; [d]ΔE_0, inner potential correction; *R* factor indicates the goodness of the fit. $S0^2$ was fixed to 0.816, according to the experimental EXAFS fit of Co foil by fixing CN as the known crystallographic value. Fitting range: $3.0 \leq k$ (/Å) ≤ 12.6 and $1.0 \leq R$ (Å) ≤ 3.0 (Co foil); $3.0 \leq k$ (/Å) ≤ 12.4 and $1.0 \leq R$ (Å) ≤ 3.5 ($Co(OH)_2$); $3.0 \leq k$ (/Å) ≤ 11.1 and $1.0 \leq R$ (Å) ≤ 3.0 (Co1); $3.0 \leq k$ (/Å) ≤ 10.1 and $1.0 \leq R$ (Å) ≤ 3.0 (Co2). A reasonable range of EXAFS fitting parameters: $0.700 < S_0^2 < 1.000$; $CN > 0$; $\sigma^2 > 0$ Å^2; $\Delta E_0 < 10$ eV; *R* factor < 0.02.

Table S4. Co-O bond lengths of TJU-28(Co) from SCXRD data.

Atom	Atom	Length (Å)
Co1	O2	2.033(5)
Co1	O4	2.096(5)
Co1	O7	2.128(5)
Co2	O1	2.045(6)
Co2	O2	2.061(5)
Co2	O3	2.148(5)
Co2	O4	2.183(5)
Co2	O5	2.071(6)
Co3	O4	2.368(5)

Table S5. Control experiments data in catalytic oxidation of ethylbenzene and tetralin.

Entry	Substrate	Catalyst	Yield (%)
1[a]	Ethylbenzene	TJU-28(Ni)	10
2		TJU-28($Co_{0.9}Ni_{0.1}$)	54
3		TJU-28($Co_{0.95}Ni_{0.05}$)	58
4[b]		TJU-28(Co) nanosheets	3
5[c]		TJU-28(Co) nanosheets	5
6[d]		TJU-28(Co) nanosheets	18
7		blank	2
8[b]	Tetralin	TJU-28(Co) nanosheets	4
9[c]		TJU-28(Co) nanosheets	5
10[d]		TJU-28(Co) nanosheets	15

[a] Reaction conditions: 8 mmol substrate, 10 mg of catalyst, 12 h, O_2 (0.5 MPa), 100 ℃ for ethylbenzene and 120 ℃ for tetralin, 66 μL (3 mol%) TBHP as the initiator. [b] Reaction under air conditions. [c] Reaction at room temperature. [d] Reaction for 2 h.

Table S6. Summary of Co-based materials for C-H oxidation.

Materials	Substrate	Condition	Yield (%)	Selectivity (%)	Ref.
$CoBr_2$	ethylbenzene	AcOH, 35% aq. H_2O_2, 80 °C	96	74	S6
Co^{II} incorporated into disordered mesoporous silicates	ethylbenzene	10 mmol TBHP, 80 °C	38	74	S7
Co-porphyrinic MOF	ethylbenzene	0.037 mmol NHPI, O_2, 60 °C	26	88	S8
ZIF-9(Co) [Co(2-pymo)$_2$]	tetralin	O_2, 90 °C	23	/	S9
Co-MOF [Co^{II}_4O(3,5-dmpz)$_6$]	cyclohexene	8 mmol TBHP, 70 °C	28	66	S10
CoAl-LDH nanosheets supported on GO	benzyl alcohol	DMF, O_2, 120 °C	92	99	S11
TJU-28(Co) nanosheets	**ethylbenzene**	**3 mol% TBHP, O_2, 100 °C**	**76**	**86**	**this study**

Table S7. Co content in the solutions after oxidation reaction (Unit: ppm).

Substrate	Ethylbenzene		Tetralin	
Catalyst	TJU-28(Co)	TJU-28(Co) Nanosheets	TJU-28(Co)	TJU-28(Co) Nanosheets
1st cycle	6.98	2.20	0.53	0.85
2nd cycle	7.29	0.95	1.08	0.12

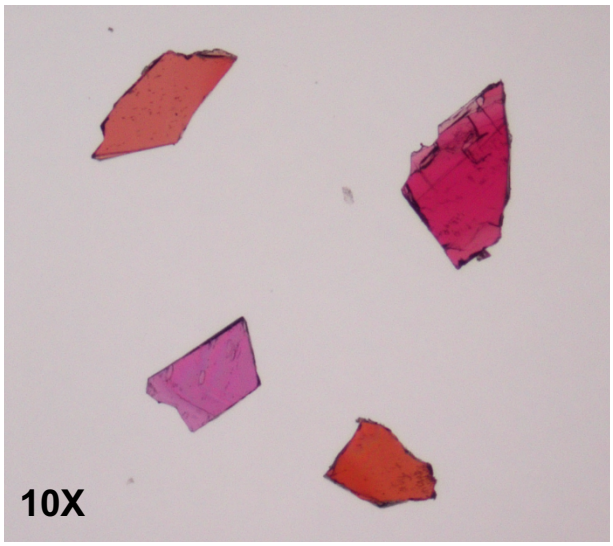

Figure S1. Optical image of as-synthesized TJU-28(Co) single crystals.

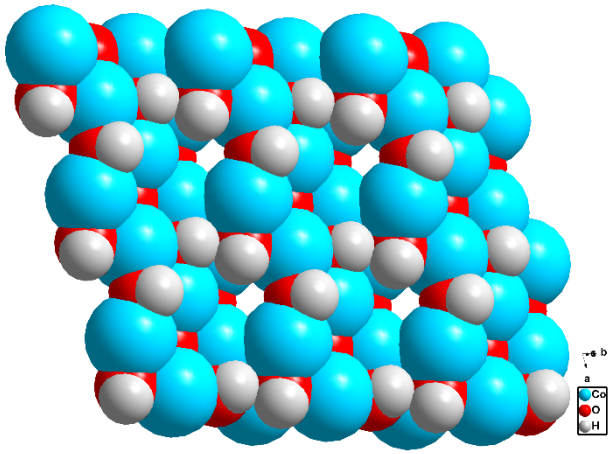

Figure S2. Space-filling model crystallographic view of inorganic layer in TJU-28(Co).

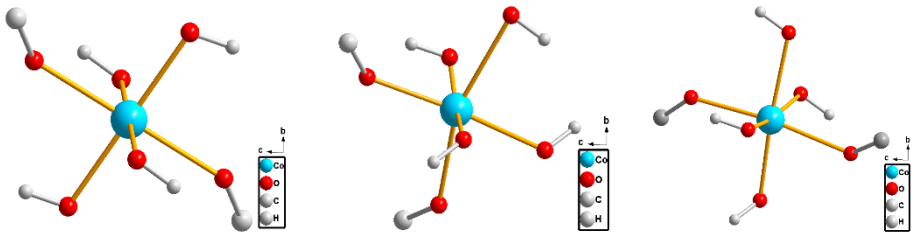

Figure S3. Crystallographic view of three independent Co^{2+} in TJU-28(Co).

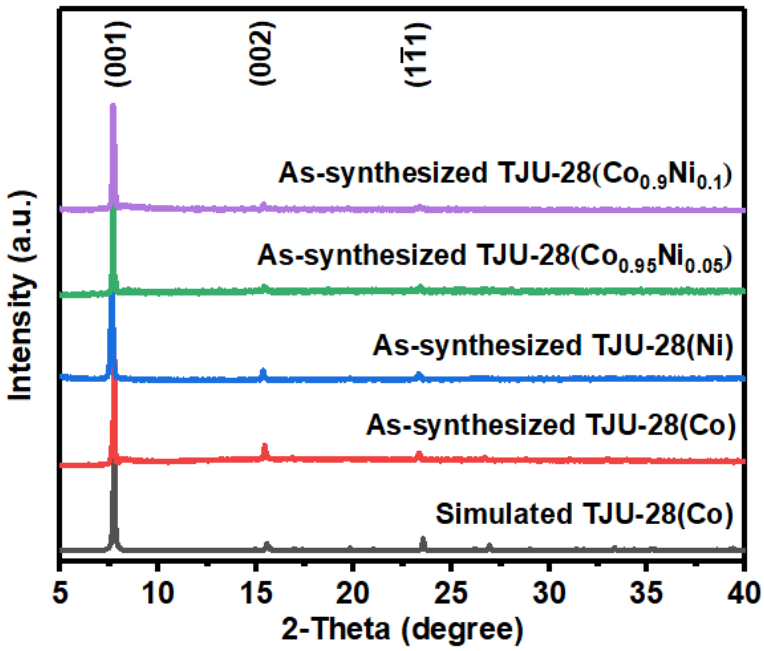

Figure S4. Power X-ray diffraction (PXRD) patterns and simulated pattern of as-synthesized TJU-28.

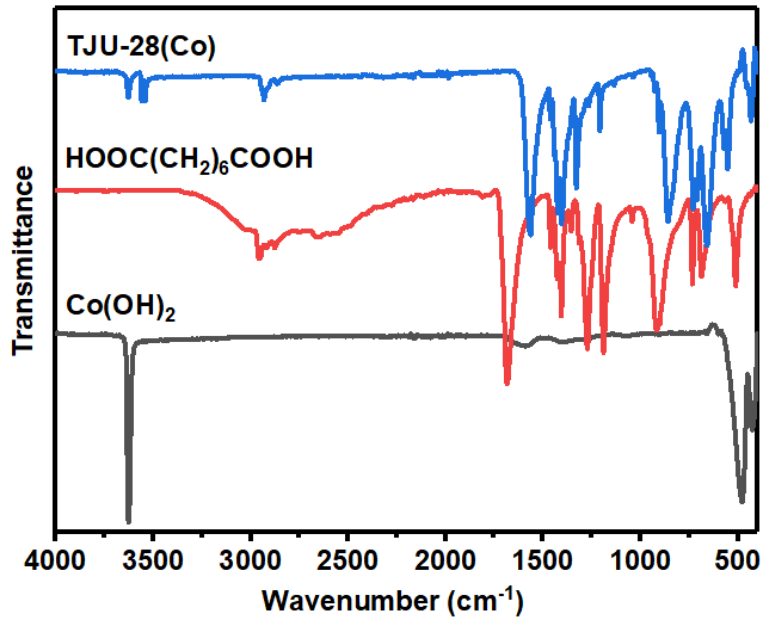

Figure S5. FTIR spectrum of synthesized TJU-28(Co), adipic acid ($HOOC(CH_2)_6COOH$) and $Co(OH)_2$.

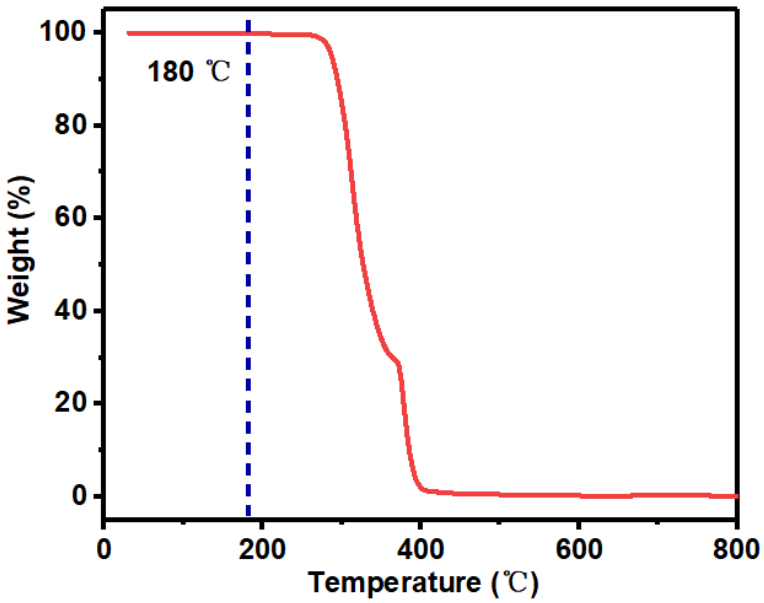

Figure S6. Thermogravimetric analysis of TJU-28(Co) under N_2 flow.

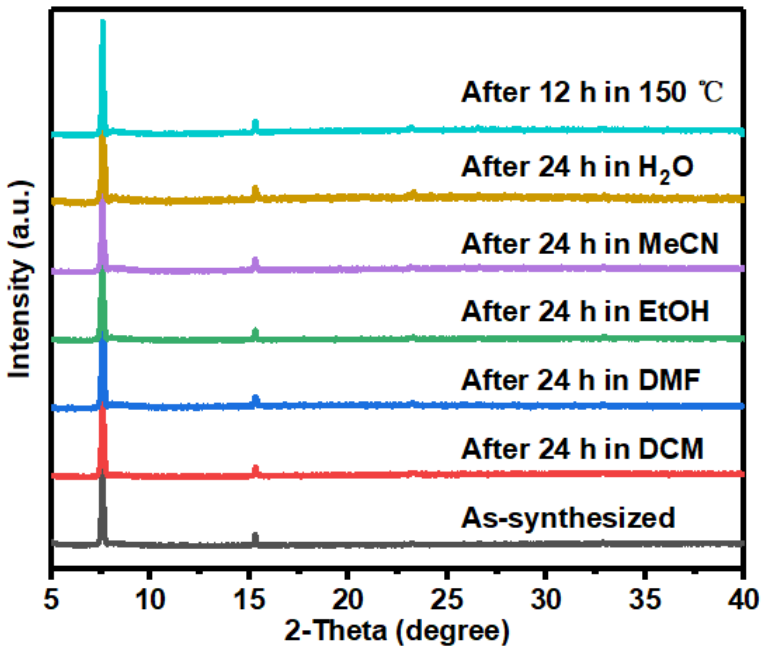

Figure S7. PXRD patterns of TJU-28(Co) before and after incubation in different solvents for 24 h and the thermal treatment at 150 °C in air for 12 h.

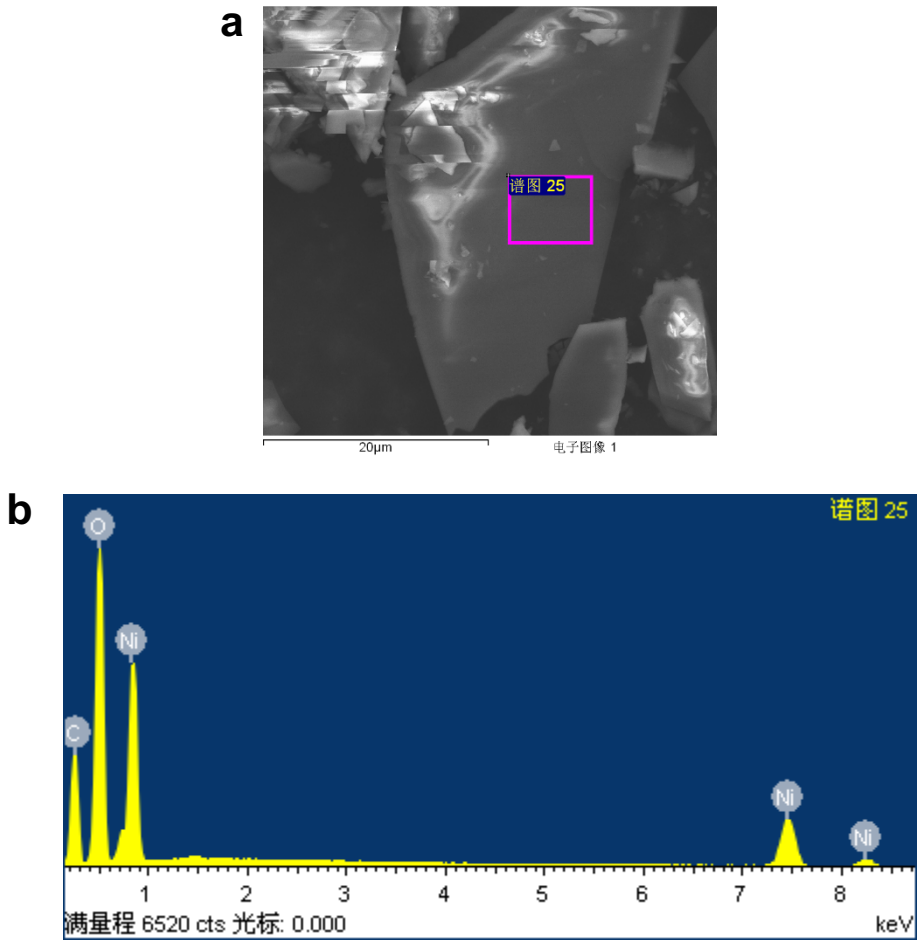

Figure S8. EDS analysis of TJU-28(Ni).

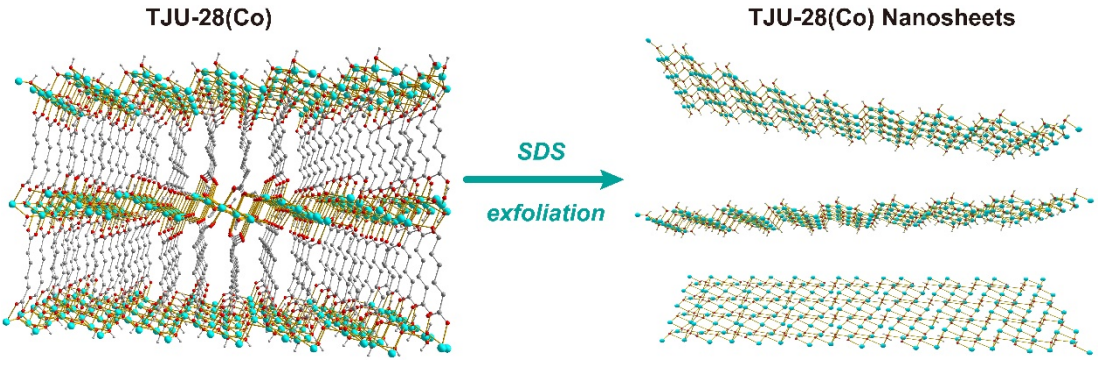

Figure S9. Schematic illustration of the exfoliation process for TJU-28(Co).

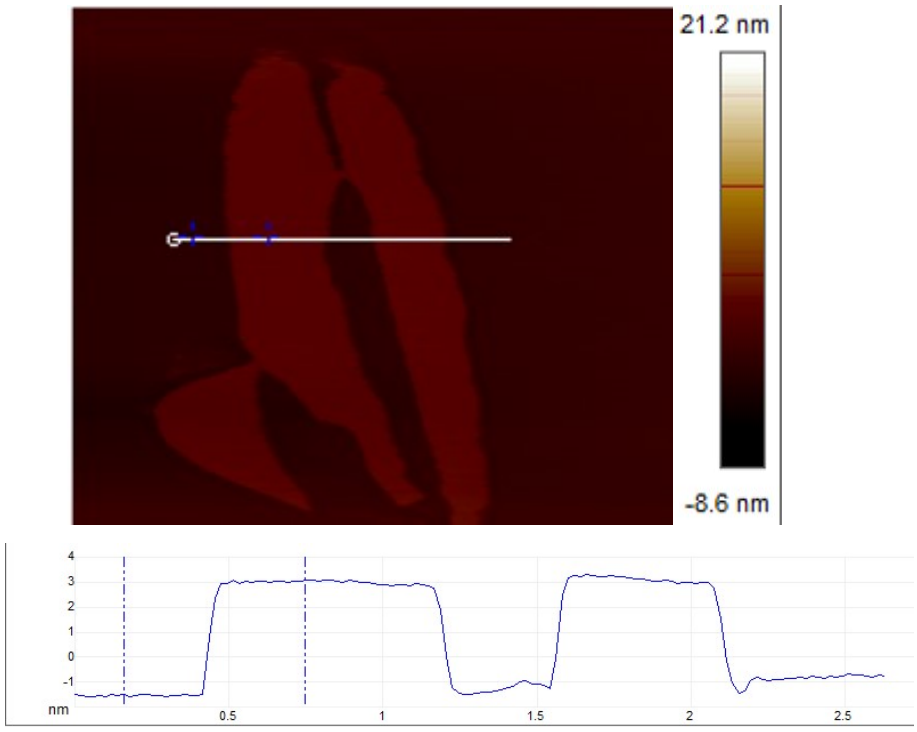

Figure S10. AFM image and height profile of TJU-28(Co) nanosheets.

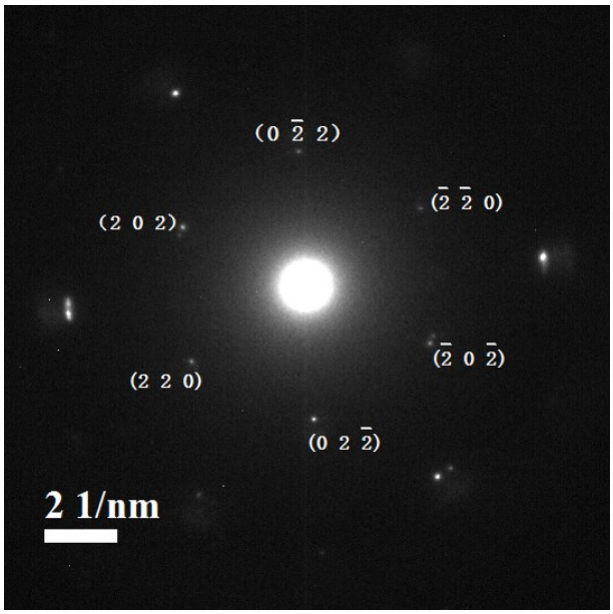

Figure S11. SAED of TJU-28(Co) nanosheets.

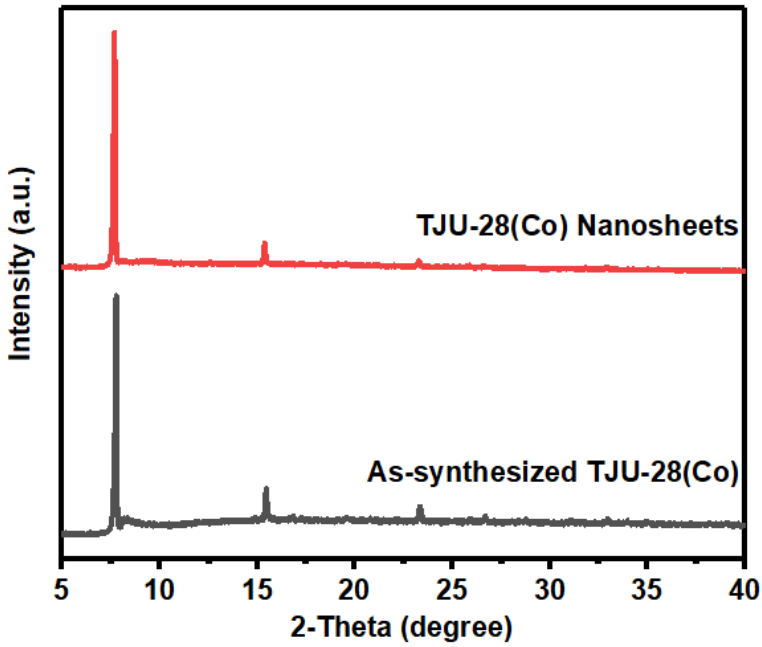

Figure S12. PXRD patterns of as-synthesized TJU-28(Co) (black) and TJU-28(Co) nanosheets (red).

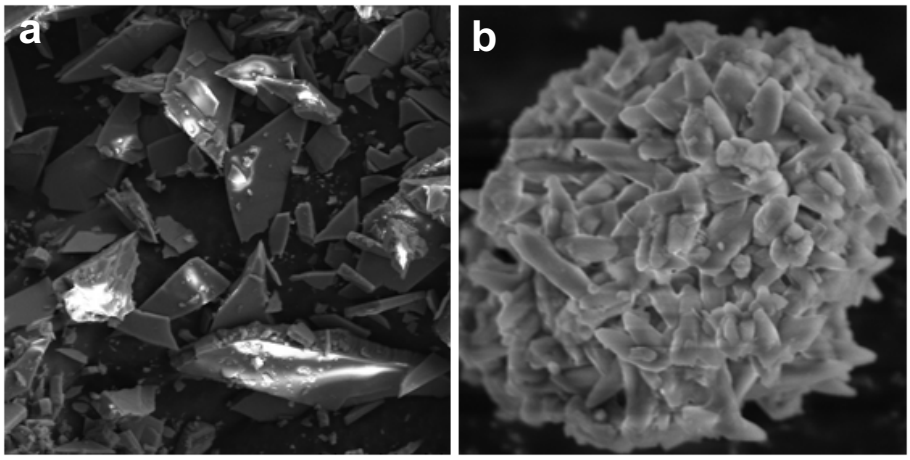

Figure S13. SEM image of TJU-28(Ni) (a) before and (b) after exfoliated by SDS.

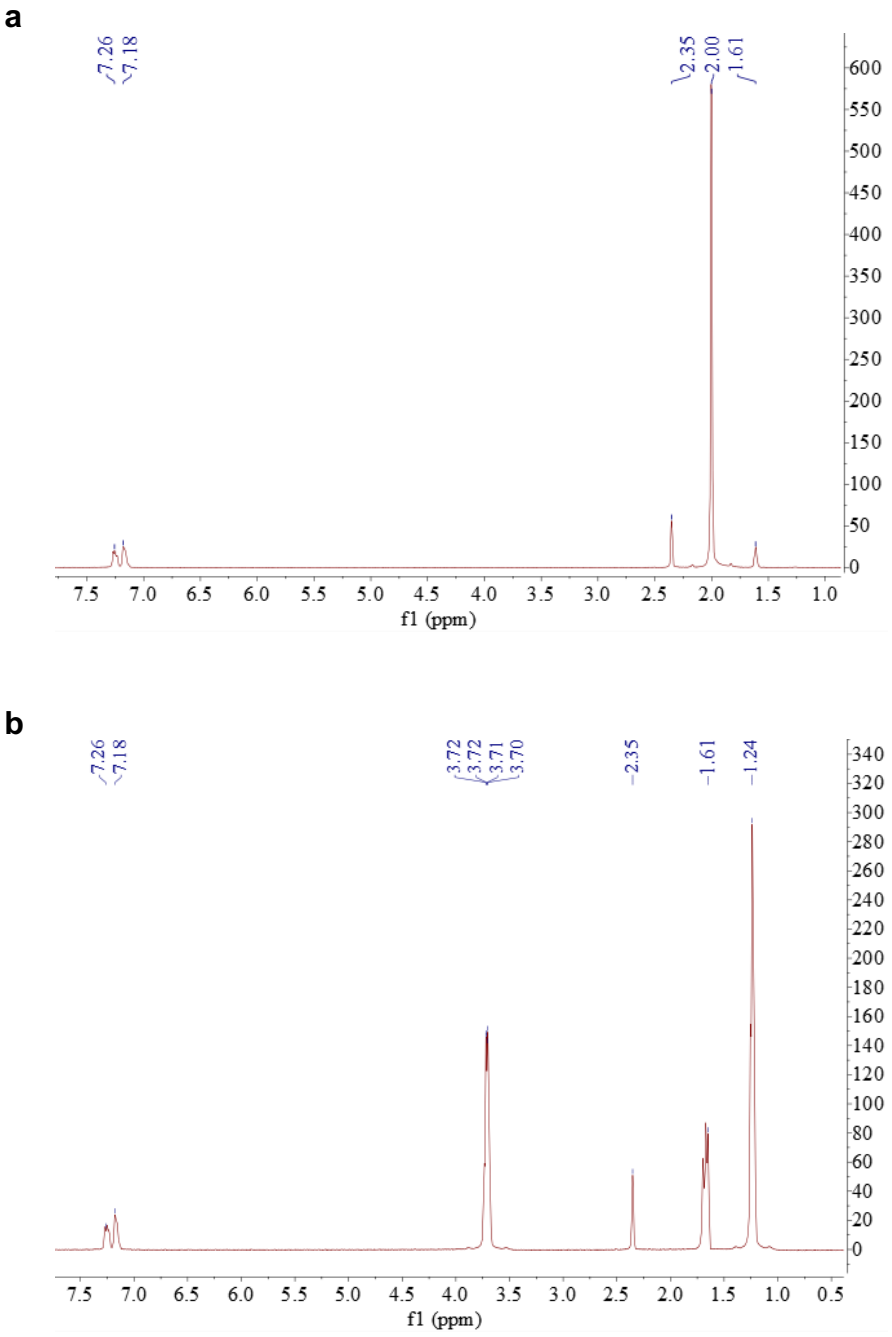

Figure S14. [1]HNMR spectrum after soaking TJU-28(Co) nanosheets in (a) acetonitrile and (b) ethanol for 2 days in CD_3Cl-d_3 with 5 μL toluene as internal standard. (toluene δ 7.18 (m, 5H), δ 2.35 (s, 1H); acetonitrile δ 2.00 (s, 3H); H_2O δ 1.61 (s, 2H); ethanol δ 3.72 (q, 2H), δ 1.24 (t, 3H))

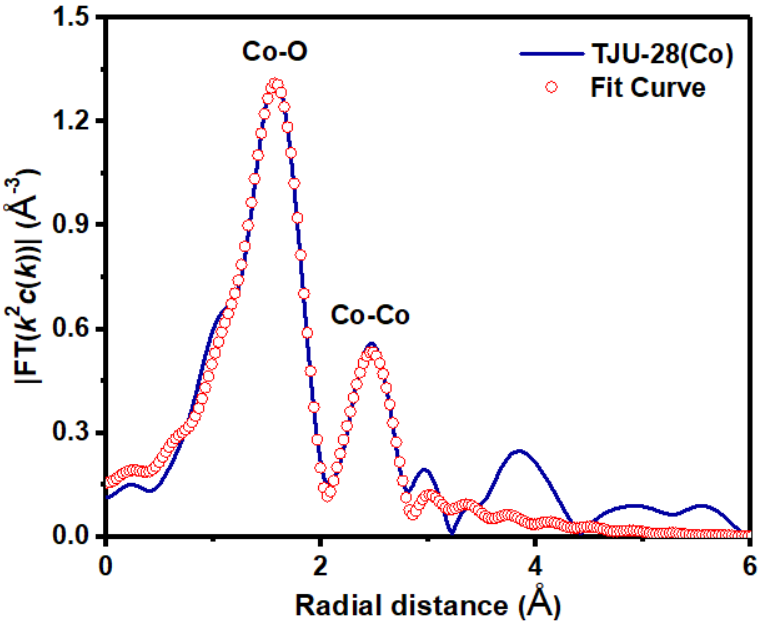

Figure S15. Co K-edge EXAFS spectra and fit curve for TJU-28(Co).

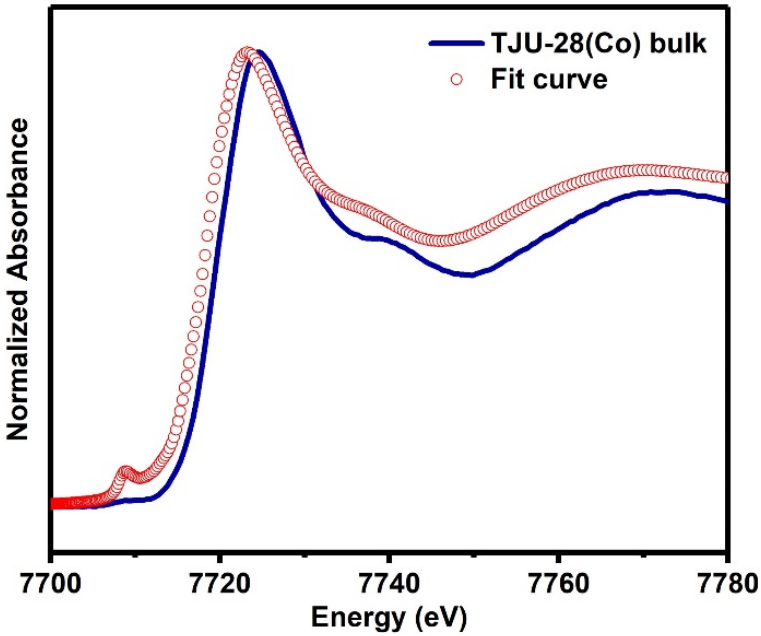

Figure S16. Comparison between the K-edge EXNES experimental spectrum of TJU-28(Co) bulk and the theoretical spectrum calculated from single-crystal data.

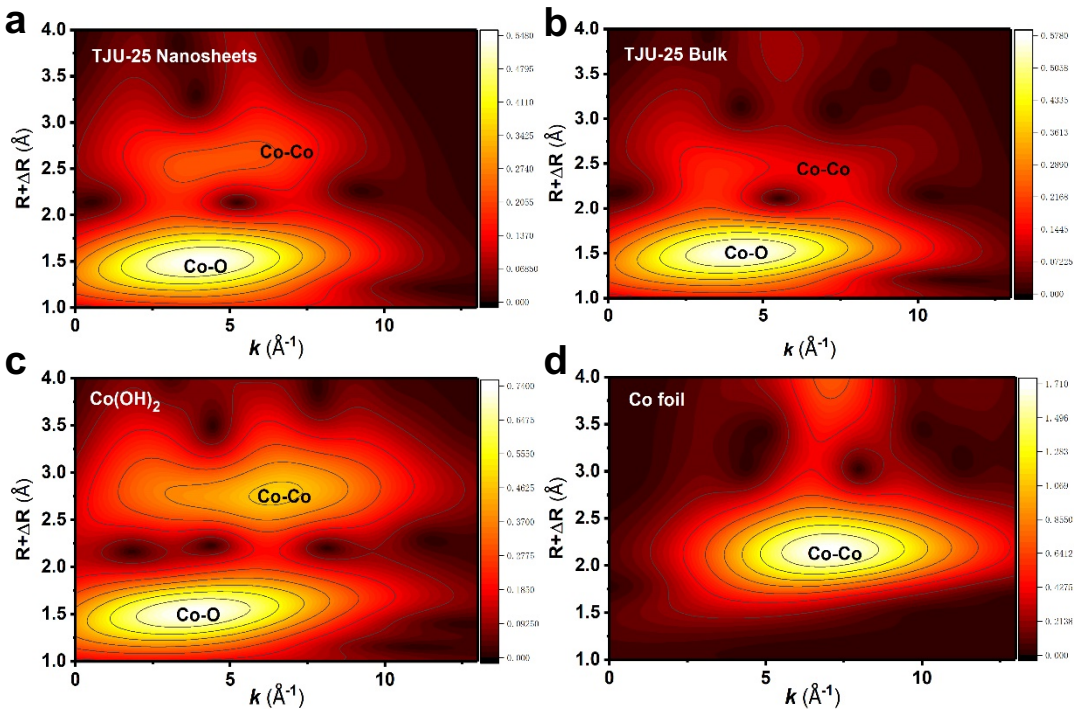

Figure S17. Co K-edge EXAFS wavelet transforms of (a)TJU-28(Co) nanosheets, (b) TJU-28(Co) bulk, (c) $Co(OH)_2$ and (d) Co foil.

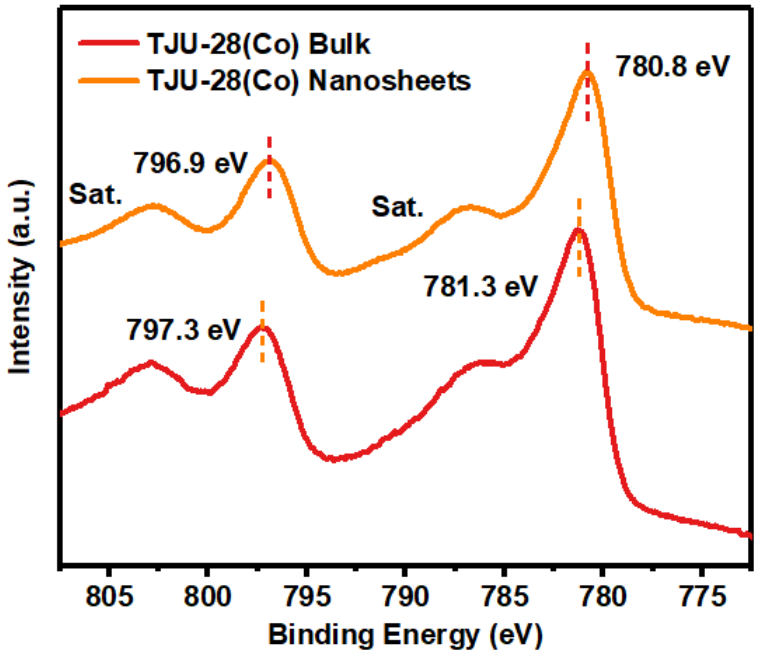

Fig S18. Co 2*p* XPS spectrum of (a) TJU-28(Co) bulk and (b) nanosheets.

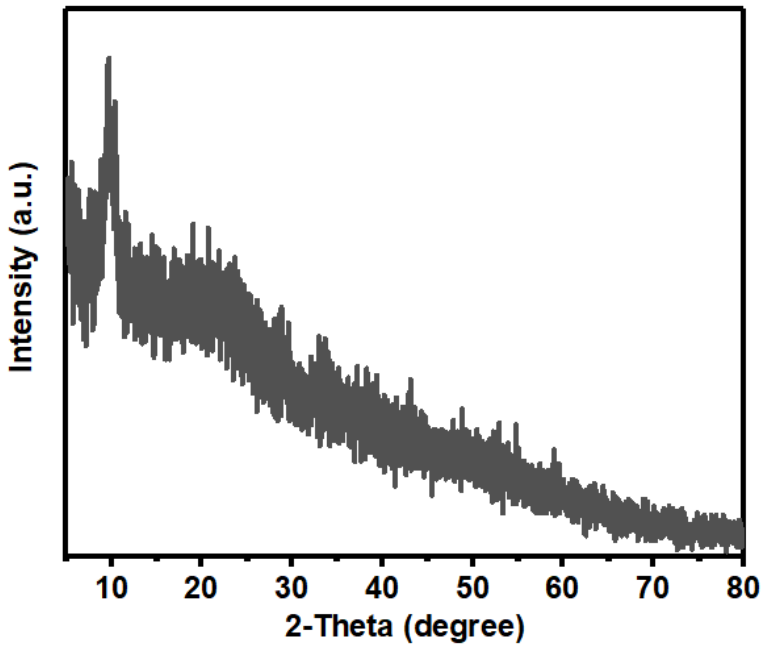

Figure S19. PXRD patterns of synthesized Co-based LDH (NiCo-LDH) according to the previous literature. [S12]

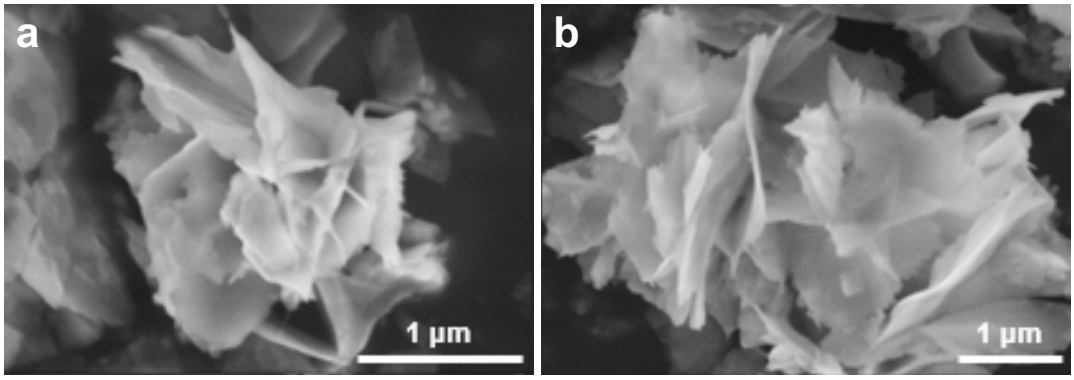

Figure S20. SEM images of TJU-28(Co) nanosheets after two oxidation cycles of ethylbenzene (a) and tetralin (b).

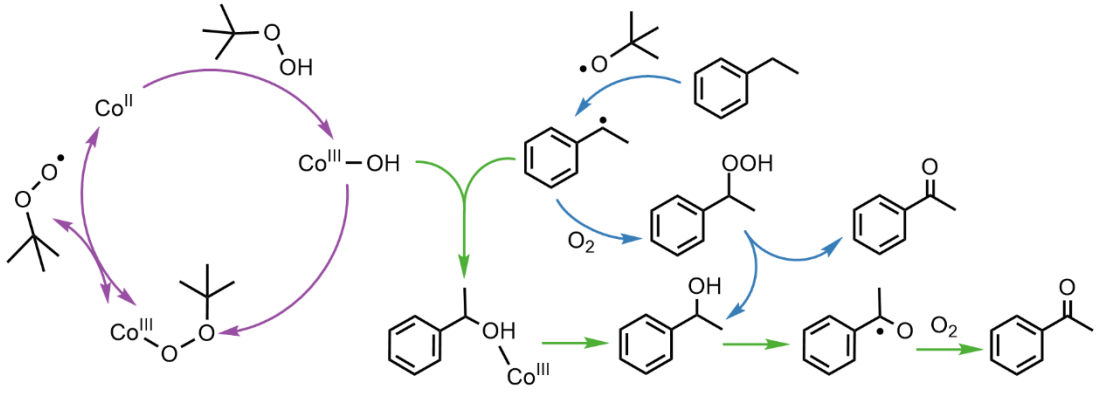

Figure S21. Plausible mechanistic pathway for ethylbenzene oxidation over TJU-28(Co).

Supporting Information References

S1. APEX-II, 2.1.4, Bruker-AXS: Madison, WI, **2007**.

S2. SHELXTL, Crystal Structure Determination Package, Bruker Analytical X-ray Systems Inc.: Madison, WI, **1995~99**.

S3. Brandenburg, K.; Putz, H., Diamond, Crystal Impact, Bonn, Germany, **2007**.

S4. Ravel, B.; Newville, M., Athena, artemis, hephaestus: data analysis for X-ray absorption spectroscopy using IFEFFIT. *Journal of Synchrotron Radiation* **2005**, 12 (4), 537-541.

S5. Funke, H.; Scheinost, A. C.; Chukalina, M., Wavelet analysis of extended x-ray absorption fine structure data. *Physical Review B* **2005**, 71 (9), 094110.

S6. Gutmann, B.; Elsner, P.; Roberge, D.; Kappe, C. O., Homogeneous liquid-phase oxidation of ethylbenzene to acetophenone in continuous flow mode. *ACS Catalysis* **2013**, 3 (12), 2669-2676.

S7. Pachamuthu, M. P.; Rajalakshmi, R.; Maheswari, R.; Ramanathan, A., Direct glycol assisted synthesis of an amorphous mesoporous silicate with framework incorporated Co^{2+}: characterization and catalytic application in ethylbenzene oxidation. *RSC Advances* **2014**, 4 (56), 29909-29916.

S8. Liu, G.; Cui, H.; Wang, S.; Zhang, L.; Su, C.-Y., A series of highly stable porphyrinic metal–organic frameworks based on iron–oxo chain clusters: design, synthesis and biomimetic catalysis. *Journal of Materials Chemistry A* **2020**, 8 (17), 8376-8382.

S9. Llabrés i Xamena, F. X.; Casanova, O.; Galiasso Tailleur, R.; Garcia, H.; Corma, A., Metal organic frameworks (MOFs) as catalysts: A combination of Cu^{2+} and Co^{2+} MOFs as an efficient catalyst for tetralin oxidation. *Journal of Catalysis* **2008**, 255 (2), 220-227.

S10. Tonigold, M.; Lu, Y.; Bredenkötter, B.; Rieger, B.; Bahnmüller, S.; Hitzbleck, J.; Langstein, G.; Volkmer, D., Heterogeneous catalytic oxidation by mfu-1: a cobalt(ii)-containing metal–organic framework. *Angewandte Chemie International Edition* **2009**, 48 (41), 7546-7550.

S11. Wang, Q.; Chen, L.; Guan, S.; Zhang, X.; Wang, B.; Cao, X.; Yu, Z.; He, Y.; Evans, D. G.; Feng, J.; Li, D. Ultrathin and vacancy-rich CoAl-layered double hydroxide/graphite oxide catalysts: promotional effect of cobalt vacancies and oxygen vacancies in alcohol oxidation. *ACS Catalysis* **2018**, 8 (4), 3104-3115.

S12. Li, R.; Hu, Z.; Shao, X.; Cheng, P.; Li, S.; Yu, W.; Lin, W.; Yuan, D., Large scale synthesis of NiCo layered double hydroxides for superior asymmetric electrochemical capacitor. *Scientific Reports* **2016**, 6 (1), 18737.